Research on the Hovering Depth Estimation of AUV Based on Multi-Sensor Fusion

Jiwei Zhao, Jiacheng Xin*, Dong Wang, Xiaoyu Zhao, Kai Chen
Tianjin Hanhai Lanfan Marine Technology Co., Ltd., Tianjin, China.
**Corresponding Author*

Abstract: Confronting the challenge faced by micro autonomous underwater vehicles (AUVs) during their hovering and depth-holding maneuvers-where they are vulnerable to the disruptive forces of ocean waves, causing the pressure readings from sensors to deviate from the true water depth pressures and consequently yielding inaccurate depth measurements-this paper unveils an innovative solution. It introduces a sophisticated method that harnesses the power of Kalman filtering for data fusion, a technique designed to elevate the precision of AUV depth measurement information to unprecedented levels. By seamlessly integrating data streams from dual pressure sensors with the acceleration values garnered from the inertial measurement unit (IMU), this method endeavors to capture the nuanced fluctuations in the AUV's actual depth with remarkable accuracy. It is as if the AUV is equipped with a heightened sense of awareness, allowing it to navigate the depths with a newfound precision and confidence. Through a series of rigorous simulation experiments, the efficacy of this algorithm is resoundingly verified. It demonstrates an exceptional capability to diminish the measurement errors associated with depth information, achieving a level of accuracy that is both impressive and invaluable. As such, this method holds immense promise for practical engineering applications.

Keywords: Micro and Small AUV; Pressure Sensor; Kalman Filter; Information Fusion

1. Introduction

In the wake of escalating global interest in marine resources and the relentless march of oceanic development, Autonomous Underwater Vehicles (AUVs) have emerged as indispensable instruments in the quest for underwater exploration, capturing the spotlight of scientific and industrial communities alike [1]. Among the array of technologies that empower AUVs to navigate the intricate depths of the ocean, the ability to maintain precise depth-holding and hover with unwavering stability stands out as a linchpin, drawing ever-increasing fascination and research endeavors. AUVs endowed with these sophisticated depth-control capabilities distinguish themselves from their peers, offering a plethora of advantages that transcend conventional boundaries. Their versatility knows no bounds, as they seamlessly transition between vast expanses of open water and confined areas, executing meticulous observations and tasks with unparalleled precision over specified durations. Whether it's delving into the mysteries of the deep sea, salvaging treasures from the ocean floor, or engaging in other specialized underwater activities, these AUVs rely on their robust hovering prowess to ensure mission success. To attain the pinnacle of depth control accuracy, the fidelity of depth information emerges as an indispensable cornerstone. In the tumultuous realm of complex underwater environments, external perturbations can wreak havoc on depth measurements, casting a shadow of uncertainty over the vehicle's control stability [2,3].

Constrained by their diminutive stature, micro and miniature Autonomous Underwater Vehicles (AUVs) are inherently limited in the sensor payload they can accommodate, with the majority of these sensors being of the Micro-Electro-Mechanical Systems (MEMS) variety, which, by their very nature, offer a degree of precision that is less than optimal. Presently, the standard practice for depth measurement in AUVs revolves around the utilization of a solitary pressure sensor. However, given the predilection of these diminutive AUVs for deployment in the shallow waters of coastal rivers and inland lakes, they find themselves particularly vulnerable to the perturbations of wave interference, a phenomenon that can significantly impact the pressure sensor's readings, leading to inaccuracies in depth perception. The reliance on a single pressure sensor for depth estimation thus presents a formidable challenge in the quest to achieve sustained and stable depth-holding and hovering control for AUVs [4,5].

In response to the quandary of imprecise depth information that plagues the depth-holding and hovering endeavors of micro and miniature AUVs, this paper delves into a comprehensive investigation, centering its focus on the "Zhifan" platform-a micro and miniature AUV par excellence. It puts forth an innovative proposition: the installation of dual pressure sensors aboard the AUV, coupled with the sophisticated application of Kalman filtering to seamlessly integrate this data with acceleration values garnered from the Inertial Measurement Unit (IMU). This fusion of data, a testament to the marriage of cutting-edge technology and meticulous engineering, serves to elevate the measurement accuracy of the micro and miniature AUV to unprecedented heights. Moreover, to ascertain the efficacy and superiority of the proposed system, a series of simulations are meticulously orchestrated, mimicking the ever-changing oceanic environmental conditions at various depths, thereby providing a robust validation of the system's capabilities.

2. Overall Scheme and Power Layout

2.1 Overall Scheme

The depth estimation system of a micro or miniature Autonomous Underwater Vehicle (AUV) is a sophisticated ensemble of integral components, chiefly encompassing sensor signal acquisition, an acceleration computation controller, and a depth calculation controller. A comprehensive schematic of the system's architectural design is elegantly depicted in Figure 1. This system harnesses the capabilities of an Inertial Measurement Unit (IMU) and dual pressure sensors for data acquisition, wherein the IMU imparts acceleration data that is seamlessly integrated with the depth information emanating from the two pressure sensors.

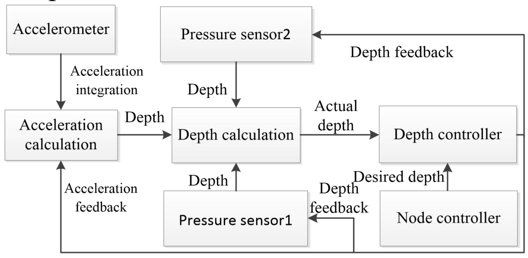

Figure 1. System Overall Design Block Diagram

2.2 Power Layout

The "Zhifan" AUV's remarkable ability to maintain depth and hover with precision is attributed to its adept utilization of bow and stern channel thrusters. The propulsion architecture is meticulously divided into two distinct sections: the channel module, which cradles two thrusters-one horizontal, designed to generate lateral thrust, and one vertical, engineered to produce thrust in the vertical plane; and the stern module, where four thrusters are arranged in a cruciform pattern, each separated by an axial angle of 45° . To achieve the pinnacle of depth-holding and hovering, the "Zhifan" AUV relies on the thrust generated by thrusters 1 and 2 in the stern module (T1 and T2) and the thrust produced by the vertical channel thruster (T5) to meticulously control the vehicle's vertical motion. Through the masterful orchestration of these thrust forces, the AUV attains a state of stable depth-holding and hovering, as vividly illustrated in Figure 2.

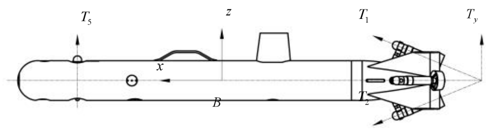

Figure 2. Power Distribution of AUV in Vertical Motion

2.3 Kinematic Model of AUV Hovering and Depth-Keeping

To achieve the depth-keeping hovering of the AUV, first, a kinematic model of the AUV's depth-keeping motion needs to be established. Assume that the mass of the AUV is m , the center of gravity is G , the navigation speed is V (u,v,w) , the angular velocity is (p,q,r) , the external force acting on it is F (X,Y,Z) , and the moment of the external force about the center of gravity is M (K,M,N) .

$$\begin{bmatrix} m-X_{\dot{u}} & -X_{\dot{w}} & mz_g-X_{\dot{q}} \\ -X_{\dot{w}} & m-Z_{\dot{w}} & -mx_g-Z_{\dot{q}} \\ mz_g-X_{\dot{q}} & -mx_g-Z_{\dot{q}} & I_y-M_{\dot{q}} \end{bmatrix}\begin{bmatrix} \dot{u} \\ \dot{w} \\ \dot{q} \end{bmatrix}$$

$$+\begin{bmatrix} -X_u & -X_w & -X_q \\ -Z_u & -Z_w & -Z_q \\ -M_u & -M_w & -M_q \end{bmatrix}\begin{bmatrix} u \\ w \\ q \end{bmatrix}+\begin{bmatrix} 0 \\ 0 \\ BG_zW\sin\theta \end{bmatrix}+ \quad (1)$$

$$\begin{bmatrix} 0 & 0 & (m-Z_{\dot{w}})w \\ 0 & 0 & 0 \\ (Z_{\dot{w}}-Z_{\dot{u}})w & 0 & mz_gw \end{bmatrix}\begin{bmatrix} u \\ w \\ q \end{bmatrix}=\begin{bmatrix} \tau_X \\ \tau_Z \\ \tau_M \end{bmatrix}$$

In order to streamline the complexity of the problem under consideration, this paper confines its analytical focus exclusively to vertical motion, eschewing any consideration of horizontal motion. Consequently, it delves solely into the vertical velocity within the vertical plane, under the assumption that horizontal velocity is effectively nullified. $u=u_0, w=\overline{w}=u=\overline{u}=q=\overline{q}=\delta_b=\delta_s=0$, considering that the "Zhifan" AUV is torpedo-shaped with a length-to-diameter ratio of 12:1, it can be approximately considered that the underwater vehicle is vertically symmetrical. So, $Z_0=0, M_0=0$. Then the above equations can be simplified as follows:

$$(m-Z_{W'})Z''-Z_wz'=f_z \quad (2)$$

In the formula, z is the depth function with respect to time t . $z'=dz/dt$ $z''=dw/dt$, f_z is the function representing the change in force caused by the thruster speed with respect to time t .

$$f_z=K_T\rho D^4\left(\frac{n}{60}\right)^2 \quad (3)$$

By performing a Laplace transform on the above equation, the transfer function for hovering and depth-keeping control can be obtained as follows:

$$F_H(s)=\frac{Z(s)}{F_z(s)}=\frac{1}{(m-Z_{W'})S^2-Z_ws} \quad (4)$$

3. Filter Design

3.1 Establishment of the Observation Model

3.1.1 IMU

The noise error sources inherent in an Inertial Measurement Unit (IMU) can be neatly partitioned into deterministic and stochastic components. Deterministic noise predominantly comprises constant drift and vibration errors, both of which are amenable to real-time compensation and relatively straightforward calibration. Among the myriad noise sources plaguing MEMS IMUs, random noise, particularly drift-or bias instability-emerges as the most formidable factor impinging upon precision. The measurement equation governing the IMU is succinctly articulated as follows:

$$a_w=a_0+\varepsilon_a+\omega_a \quad (5)$$

In the formula, a_w is the measured value of the IMU, a_0 is the actual speed of the AUV, ε_a is the deterministic noise, represented by white noise, and ω_a is the random noise, also represented by white noise.

3.1.2 Two pressure sensors

The noise impinging upon the pressure sensor can be categorized into intrinsic and extrinsic noise. Intrinsic noise chiefly encompasses mechanical noise and electrical noise. The mechanical noise within the system is overwhelmingly ascribed to Brownian noise, which emanates from the mechanical fluctuations of the membrane induced by Brownian forces. Conversely, the electrical noise sources are primarily composed of thermal noise (also known as Johnson noise) and 1/f noise. In comparison to thermal noise, Brownian noise can be safely disregarded. It is the electrical noise that imposes stringent limitations upon the sensor's minimum resolution [6].

Extrinsic noise predominantly originates from external environmental perturbations, with particular significance attributed to those encountered by an Autonomous Underwater Vehicle (AUV) as it traverses varying depths in aquatic environments. In proximity to the water's surface, the pressure sensor is chiefly susceptible to the impact of oceanic waves, which engender discrepancies between the measured pressure values and the actual pressure corresponding to the water depth, thereby casting a shadow of uncertainty over the precision of depth measurements. Conversely, when operating in the relative tranquility of deeper waters, the AUV finds itself largely shielded from the tumultuous influence of surface currents and waves, with the pressure sensor primarily succumbing to transient disturbances such as surges.

Therefore, the measurement equation of the pressure sensor is as follows:

$$d_w = d_0 + \varepsilon_b + \omega_s \tag{6}$$

In the formula, d_w is the measurement value of the pressure sensor, d_0 is the actual depth of the Autonomous Underwater Vehicle (AUV), ε_b is the intrinsic noise of the pressure sensor, which is represented by white noise, and ω_s is the extrinsic noise. Near the water surface, it is the wave interference. The waves are colored noise. In relatively deeper areas, it is the instantaneous interference, which is considered as a random error [7].

Two pressure sensors are used on the Zhifan AUV. Therefore, we assume that the measured values of the two distance measurement sensors are h_{w1} and h_{w2} respectively, and the noises of the pressure sensors themselves are ε_{b1} and ε_{b2} respectively. The measurement sampling period is cc. Among them, the noises themselves are represented by white noise with zero mean value. That is, the measurement equations of the two pressure sensors are obtained:

$$h_{w1} = h_0 + \varepsilon_{b1} \tag{7}$$

$$h_{w2} = h_0 + \varepsilon_{b2} \tag{8}$$

The observed outputs of the state equation include acceleration and two depth values

$$Y(k) = \begin{bmatrix} P_1(k) \\ P_2(k) \\ a(k) \end{bmatrix} \tag{9}$$

The relationship between the pressure value and the depth value is

$$\begin{bmatrix} P_1(k) \\ P_2(k) \\ a(k) \end{bmatrix} = \begin{bmatrix} 1 & 0 & 0 \\ 1 & 0 & 0 \\ 0 & 0 & 1 \end{bmatrix} \begin{bmatrix} h_1(k) \\ h_2(k) \\ a(k) \end{bmatrix} + \begin{bmatrix} \varepsilon_{b1} \\ \varepsilon_{b2} \\ \varepsilon_{\mathrm{a}} \end{bmatrix} \tag{10}$$

Derive

$$H = \begin{bmatrix} 1 & 0 & 0 \\ 1 & 0 & 0 \\ 0 & 0 & 1 \end{bmatrix} \tag{11}$$

$$V = \begin{bmatrix} \varepsilon_{b1} \\ \varepsilon_{b2} \\ \varepsilon_{\mathrm{a}} \end{bmatrix} \tag{12}$$

3.2 System Model

In the pursuit of designing a Kalman filter, it is of paramount importance to first erect a formidable system state equation. The discrete state equation of the system unfolds as follows:

$$X(k+1) = \Phi X_k + Bu_k + \Gamma W_k \tag{13}$$

$$Y(k) = HX(k) + V(k) \tag{14}$$

In Equations (12) and (13), $X(k)$ represents the current state, $X(k+1)$ represents the state at the next moment, Φ is the transition matrix, B is the control matrix, u is the control quantity, Γ is the noise matrix, $W(k)$ is the system noise, $Y(k)$ is the output quantity, H is the output matrix, and $V(k)$ is the observation noise.

In Equation (14), $X(k)$ represents a vector that includes acceleration, velocity, and altitude. The equation is as follows:

$$X(k) = \begin{bmatrix} h(k) \\ v(k) \\ a(k) \end{bmatrix} \tag{15}$$

In the same way

$$X(k+1) = \begin{bmatrix} h(k+1) \\ v(k+1) \\ a(k+1) \end{bmatrix} \tag{16}$$

In Equations (15) and (16)

$X(k)$ represents the current state, and $h(k), v(k), a(k)$ respectively represent the acceleration, velocity and altitude under the current state.

$h(k+1), v(k+1), a(k+1)$ encapsulates the acceleration, velocity, and altitude at the succeeding time step. The state transition matrix, Φ, stands as a sentinel matrix that elucidates the intricate relationship between the state at the impending time step and the state at the present time step. Within this system, we possess the clarity to demarcate their interdependence with precision. Assuming a sampling period, T, of relatively brief duration, it can be reasonably approximated that the acceleration remains steadfastly constant.

Derive

$$\begin{bmatrix} h(k+1) \\ v(k+1) \\ a(k+1) \end{bmatrix} = \begin{bmatrix} 1 & T & 0.5T^2 \\ 0 & 1 & T \\ 0 & 0 & 1 \end{bmatrix} \begin{bmatrix} h(k) \\ v(k) \\ a(k) \end{bmatrix} \tag{17}$$

It can be obtained that the transition matrix Φ is

$$\phi = \begin{bmatrix} 1 & T & 0.5T^2 \\ 0 & 1 & T \\ 0 & 0 & 1 \end{bmatrix} \tag{18}$$

The observed output of the state equation includes acceleration and two sets of depth values

$$Y(k)=\begin{bmatrix}P_1(k)\\P_2(k)\\a(k)\end{bmatrix} \tag{19}$$

The relationship between the pressure value and the depth value is

$$\begin{bmatrix}P_1(k)\\P_2(k)\\a(k)\end{bmatrix}=\begin{bmatrix}1&0&0\\1&0&0\\0&0&1\end{bmatrix}\begin{bmatrix}h_1(k)\\h_2(k)\\a(k)\end{bmatrix} \tag{20}$$

Derive

$$H=\begin{bmatrix}1&0&0\\1&0&0\\0&0&1\end{bmatrix} \tag{21}$$

3.3 Steps of the Depth Estimation Algorithm

1) Prediction process

Stemming from the system state equation, referred to as Equation (12), we deduce the one-step prediction of the system's state, as expressed below:

$$\hat{X}(k)=\phi\hat{X}(k-1) \tag{22}$$

In formula (22), $\hat{X}(k)$ represents the estimated value.

The predicted covariance matrix is as follows:

$$\hat{P}(k)=\phi\hat{P}(k-1)\phi^T+\Gamma Q\Gamma^T \tag{23}$$

In formula (23), the covariance matrix P is a third-order matrix. $P(K-1)$ is the previous covariance matrix, Γ is the identity matrix, Q is a third-order diagonal matrix, and each value q on the diagonal represents the process error corresponding to the three variables.

2) State update process

The calculation of the filtering gain is as follows:

$$K(k)=\hat{P}(k)H^T[H\hat{P}(k)H^T+R]^{-1} \tag{24}$$

The filtering gain matrix $K(k)$ this time is calculated from $P(K)$ obtained in the previous step, the output matrix H, and the observation noise matrix R set during the initialization.

$$R=\begin{bmatrix}r_{k1}&0&0\\0&r_{k2}&0\\0&0&r_{k3}\end{bmatrix} \tag{25}$$

In formula (25), R embodies the measurement noise matrix pertaining to the dual pressure sensors and the Inertial Measurement Unit (IMU), a matrix that encapsulates the inherent error magnitude associated with the sensor measurements.

The calculation of the optimal estimate of the current state is as follows:

$$X(k)=\hat{X}(k)+K(k)(Y(k)-H\hat{X}(k)-V) \tag{26}$$

Subsequently, the predicted state, obtained through the initial step, undergoes refinement to yield the optimal estimate for the current iteration-a crucial outcome that constitutes the depth estimate pursued in this scholarly endeavor. Herein, $Y(K)$ symbolizes the actual measurement values garnered from the sensors.

The updated state estimation covariance is as follows

$$P(k)=[1-K(k)H]\hat{P}(k) \tag{27}$$

4. Algorithm Simulation and Result Analysis

The algorithm is subjected to simulation utilizing MATLAB, a powerful tool employed to ascertain its efficacy and precision. Through a meticulous analysis of the errors embedded within the simulation results, we embark on an iterative journey of fine-tuning the filter's parameters-specifically, P_0 , R_0 , and q -in a quest to attain a resilient estimation of the state variables. This endeavor ensures that the derived depth values are not only smooth but also characterized by an exquisitely minimal error margin. The diverse modules of the algorithm simulation program, along with the intricate data flow diagram, are artistically portrayed in Figure 3.

Within the simulation framework, error models tailored to each sensor are harnessed to generate data streams from dual pressure sensors, in conjunction with acceleration data. Depth measurements emanating from the two pressure sensors are systematically gathered at one-second intervals, while the Kalman filter concurrently executes an optimal estimation through the sophisticated process of data fusion. Furthermore, the depth estimation for the micro and miniature Autonomous Underwater Vehicle (AUV) is meticulously simulated across a spectrum of operational conditions.

1) First, the simulation delves into depth estimation within the tranquil expanse of still water under ideal conditions, with the resultant findings elegantly illustrated in Figures 4 and 5.

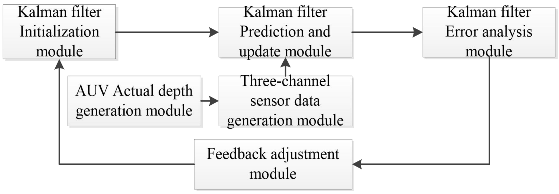

Figure 3. Algorithm Simulation Program Flow Chart

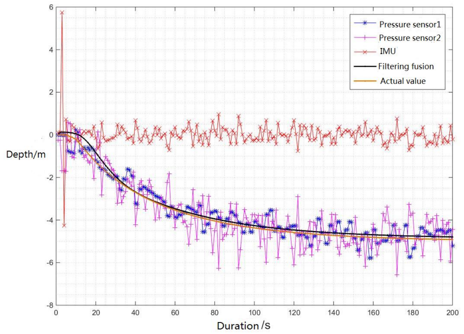

Figure 4. Results of Still Water Depth Estimation

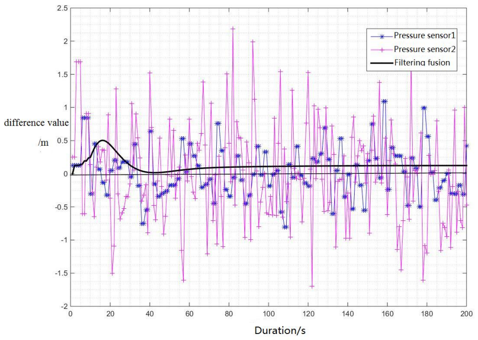

Figure 5. Contrast of Difference between Results in Still Water

A perusal of Figures 4 and 5 reveals that when dependence is placed on measurements from a solitary sensor, the noise inherent in the readings from the two pressure sensors assumes a relatively pronounced magnitude, engendering fluctuations in depth with an amplitude of 0.25 meters. However, upon the implementation of the Kalman filter data fusion algorithm for estimation purposes, the error associated with a single sensor undergoes a marked reduction. Once the AUV attains a state of stability, the error is skillfully contained within a mere 0.1 meters.

When operating in proximity to the water's surface, the AUV finds itself vulnerable to the confluence of sea waves and currents. The impact of waves upon the pressure sensors can give rise to disparities between the measured pressure values and the actual pressure corresponding to the depth, while the accelerometer may encounter vibrational noise interference. To faithfully simulate the wave interference encountered by the AUV during its motion, random signals composed of cosine functions are judiciously incorporated within the vertical plane [8]. Given that the primary sphere of operation for micro and miniature AUVs lies within nearshore diving waters, where sea conditions typically do not surpass level 3 [9], it is postulated that the AUV operates under level 3 sea conditions with an anticipated depth setting of 5 meters. The simulation results are artistically presented in Figures 6 and 7.

Scrutinizing Figures 6 and 7, it becomes apparent that, amidst level 3 sea conditions, the Autonomous Underwater Vehicle (AUV) undergoes fluctuations in tandem with the waves. The impact force of the waves engenders a deviation of 2 meters in the data emanating from the dual pressure sensors. However, following the processes of filtration and fusion, the data harmonizes seamlessly with the actual motion curve, thereby ensuring that the error margin is confined within a mere 0.3 meters once the AUV attains stability.

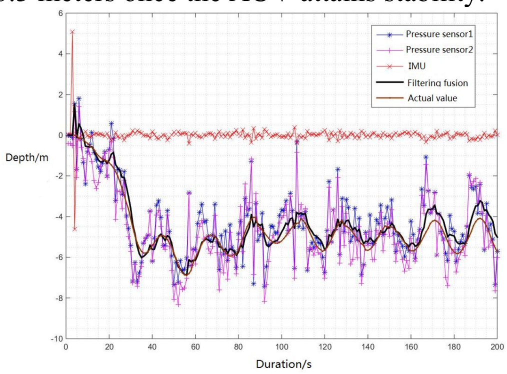

Figure 6. Simulation Results of Depth Estimation under Wave Action

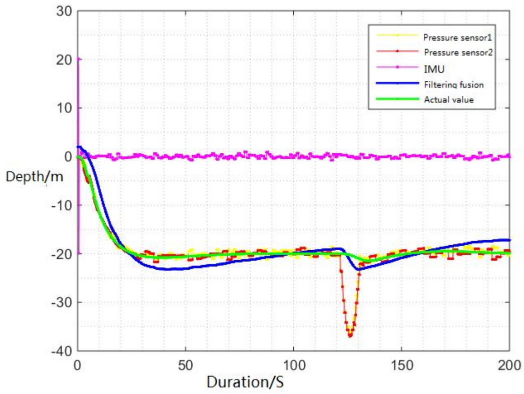

Figure 7. Error Comparison of Results under Wave Action

3) When the AUV traverses the relatively deeper expanse of waters, it remains largely impervious to the influence of surface currents

and waves. Instead, its vertical motion is predominantly swayed by transient disturbances, such as surges. To emulate the effect of surges, an instantaneous disturbance force is introduced into the simulation [10]. A disturbance force, denoted as F, with a magnitude of 50 N, is applied to perturb the pressure sensors, with the disturbance commencing at the 120-second mark and enduring for a duration of 3 seconds. The desired depth setting is established at 20 meters, and the simulation results are elegantly portrayed in Figure 8.

As depicted in Figure 8, under the sway of the surge disturbance, the AUV experiences subtle fluctuations, which induce significant deviations in the readings of the two pressure sensors. Nonetheless, after undergoing filtration and fusion, the data aligns remarkably well with the actual motion curve, thereby ensuring that the error margin is maintained within a mere 1 meter once the AUV attains stability.

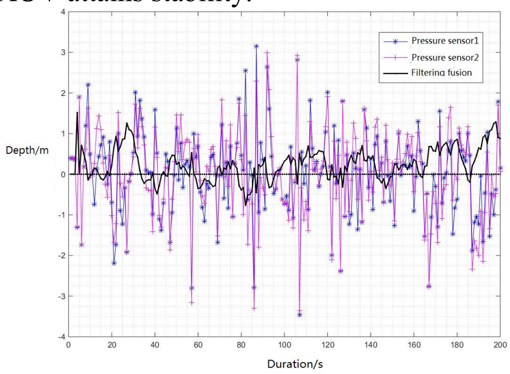

Figure 8. Simulation Results of Fixed Depth 20m Depth Estimation

5. Conclusion

This scholarly paper puts forth an optimal depth estimation algorithm, grounded in Kalman filtering, for the fusion of data derived from two pressure sensors and an Inertial Measurement Unit (IMU). The fundamental blueprint of the algorithm is unveiled, a state model is meticulously established, and the detailed execution steps of the algorithm are comprehensively outlined. Depth variation predictions are conducted for scenarios wherein the AUV is subjected to disturbances in both near-surface and relatively deeper waters. The simulation results underscore the algorithm's efficacy in seamlessly fusing the data from the two pressure sensors and the IMU, thereby significantly mitigating measurement errors. The Kalman filtering estimation algorithm proposed herein exhibits remarkable performance and holds substantial engineering application value. The subsequent step involves further refining the algorithm to enhance measurement precision and conducting practical experimental validations.

References

[1] Xinsong Jiang, Xisheng Feng, Ditang Wang. Underwater Robots. Liaoning: Liaoning Science and Technology Press, 2000.

[2] Yu Wang, Rong Zheng, Jianguo Wu. Research on the Depth Control of AUV Based on the Buoyancy Adjustment System. Automation & Instrumentation, 2015, 30(04): 6-10+15.

[3] Yu Wang, Xiutao Lin, Shijun Song, Yuhong Liu, Hongwei Zhang, Shuxin Wang. Dynamic Modeling and Simulation of a Vector Propulsion Autonomous Underwater Vehicle. Journal of Tianjin University (Science and Technology), 2014, 47(02): 143-148.

[4] HUAMING Q, QUANXI X, BO J, et al. On modeling of random drift of MEMS gyroscope and design of Kalman fifilter Proceedings of the 2009 IEEE International Conference on Mechatronics and Automation. Changchun, China: IEEE, 2009.

[5] Chenglong Xu. Research on the Navigation Method of Autonomous Underwater Vehicle (AUV) Based on Multi - Sensor Fusion. Northeastern University, 2017.

[6] Wenjun Chang, Jiancheng Liu, Huanan Yu, et al. Mathematical Model for Motion Control and Simulation of Underwater Robots. Ship Engineering, 2002 (3):

[7] Li Li. Analysis and Improvement of the Signal-to-Noise Ratio (SNR) of Piezoresistive Pressure Sensors. Electronic Test, 2014(15): 44-46.

[8] Hong'an Qiu. Establishment and Simulation Analysis of Random Ocean Wave Models. Journal of System Simulation, 2000, 12(5): 226-228.

[9] PACKARD G E, KUKULYA A, AUSTIN T, et al. Continuous autonomous tracking and imaging of white sharks and basking sharks using a REMUS-100 AUV Oceans. IEEE, 2013.

[10]Xuezhi Feng, Qiangqiang Jiang, Quanming Miao, et al. Calculation of the Motions and Wave Forces of a Submerged Body at Different Submergence Depths and Headings Near the Free Surface in Waves. Journal of Ship Mechanics, 2002, 6(2): 1-14.

